A Simple Way To Prepare PbS Nanocrystals with Morphology Tuning at Room Temperature

Zhihua Zhang, Sie Huey Lee, Jagadese J. Vittal, and Wee Shong Chin*

Department of Chemistry, National University of Singapore, 3 Science Drive 3, Singapore 117543, Singapore

Received: December 13, 2005; In Final Form: February 13, 2006

A simple way to synthesize PbS nanocrystals with the ability to tune their morphology at room temperature is reported. The preparation utilizes an amine-catalyzed decomposition of a precursor and the amine was found to play dual roles as both the catalyst and the capping agent. Spherical PbS nanocrystals of diameters 5 to 10 nm were obtained when long chain alkylamines were used in the pot. When difunctional ethylenediamine was used instead, exclusively PbS dendrites can be isolated from the same precursor at room temperature. Uniform six- and four-armed dendrites are observed, with regular branches of ∼20 nm in diameter growing in a parallel order. In a further step, morphology tuning of the dendrites to induce 1D growth into nanorods is achievable through the addition of a trace amount of stronger capping dodecanethiol molecules. Thus, PbS nanorods with aspect ratios of ∼20 to 30 could be successfully obtained and illustrated. A possible formation mechanism is discussed and the initial step of the reaction mechanism was modeled with DFT calculations as a nucleophilic attack.

Introduction

The intrinsic properties of nanomaterials are strongly determined by their crystallinity and morphologies.[1−4] Much research attention has been focused over the past few years on finding ways to conveniently control the morphologies of nanostructures during synthesis. The most common strategy is to use specific surfactants that can bind selectively to particular crystals facets; growth rates on different facets can thus be enhanced or weakened, and consequently produce nanocrystals of different morphologies. For example, it has been found that phosphonic acid, which coordinates more strongly with cadmium ion than TOPO, is essential for the generation of shape anisotropy in CdSe quantum rods.[5] Peng et al. further explored the experimental conditions and found that the growth of CdSe nanorods is a diffusion-controlled process.[6] They proposed that the size and shape of the final nanocrystals are determined by two relating factors: the magic sized nuclei and the concentration of the remaining monomers after the nucleation stage. On the other hand, multiarmed and 1D CdS nanocrystals have been obtained from the precursor method by adjusting the reaction temperature and the precursor concentration.[7] It was shown that the different phases of seeds generated at different temperatures would control the growth orientation of the final nanocrystals.

PbS (galena) is an important semiconductor due to its narrow band gap (0.41 eV) and large exciton Bohr radius (18 nm). Nanometer-sized PbS particles hence exhibit a strong quantum confinement effect and have been promising for optoelectronic devices such as sensors, IR photodetectors, flame monitors, optical switches, etc.[8] Recently, efficient multiple exciton generation has been detected in PbS quantum dots, making it a promising candidate for highly efficient photovoltaic conversion devices.[9]

Thus far, PbS nanoparticles have been prepared by arrested precipitation in micelle,[10] sol−gels,[11] glasses,[12] Langmuir−Blodgett films,[13] and polymer matrix,[14] as well as from the decomposition of single molecular precursor.[15] Most recently, PbS nanocrystals with variable sizes and shapes have also been synthesized through the thermolysis of the metal complex with sulfur at high temperatures,[16,17] and the preparation of near-IR luminescent PbS nanoparticles in aqueous solvent has been reported.[18] Meanwhile, PbS nanorods were prepared from lead salts and a sulfur source in colloidal alkyldiamine solutions.[19] Star-shaped and dendritic PbS nanocrystals have also been obtained by injecting molecular precursor into hot coordination solvent,[20] or using the surfactant-assisted hydrothermal method[21] or microwave irradiation.[22]

In this paper, we present a very simple synthesis of PbS nanocrystals with morphology-tuning to spherical particles, dendrites, and nanorods, at ambient conditions. We demonstrate that a change in morphology can be achieved readily by simple chemistry of the capping reagent. In our method, a lead thiobenzoate precursor, $Pb(SCOC_6H_5)_2$ (abbreviated as PbTB hereafter), was catalyzed by amine to decompose at room temperature. To the best of our knowledge, such breaking down of a precursor at room temperature to produce nanocrystals has not been reported before. We have recently reported the production of Ag_2S nanocubes using the analogous silver precursor by heating to 80−120 °C,[23] and also the formation of water-soluble CdS nanocrystals by refluxing the related Cd precursor in basic aqueous solution.[24] In this context, we attempted to obtain more insight of the simple precursor reaction by modeled DFT calculations.

Experimental Section

(A) Commercial Chemicals. $Pb(OOCH_3)_2 \cdot 3H_2O$ (Fluka, 99%), thiobenzoic acid (Fluka, 95%), oleylamine (Aldrich, 70%), dioctylamine (Aldrich, 98%), trioctylamine (Aldrich, 98%), ethylendiamine (Aldrich, 99%), and 1-dodecanethiol (Acros, 98%) were used as received.

(B) Preparation of Lead Thiobenzoate Precursor. PbTB-was synthesized according to a reported method.[25] A brief description of the preparation is as follows: thiobenzoic acid (5.5 mL, 46.8 mmol) was added slowly to a stirred solution of lead acetate (5.17 g, 13.6 mmol) in 30 mL of ethanol. A thick

* Address correspondence to this author. E-mail: chmcws@nus.edu.sg. FAX: 65-6779-1691.

10.1021/jp057271m CCC: $33.50
Published on Web 03/16/2006

suspension of yellow precipitate appeared immediately. The acid was added below the surface with a syringe to avoid the formation of brown contaminant, presumably PbS, and the mixture was stirred for 2 h to ensure complete reaction. The thick suspension was then centrifuged, the supernatant liquid was removed, and the solid was washed three times with cold ethanol, with centrifugation between washings. In the final cycle, the supernatant liquid was colorless. The product was dried under vacuum. Yield: 5.2 g (79.0%). Melting point: 163−165 °C. Anal. Calcd for $C_{14}H_{10}O_2S_2Pb$: C 34.92, H 2.09, S 13.31. Found: C 34.89, H 2.00, S 13.45. ^{1}H NMR (DMSO): δ 7.47 (t, 2H), δ 7.60 (t, 1H), δ 8.03 (d, 2H).

(C) Preparation of PbS Spherical Nanoparticles from Monofunctionl Amines. PbTB (50 mg, 0.1 mmol) was added into a flask, followed by the injection of 1.2 mmol of amine (oleylamine/dioctylamine/trioctylamine). It is noted that the Pb-to-amine feed ratio can be optimized for different amines but the ratio was kept constant here at 1:12 for consistent comparison. After the mixture was stirred for about 30 min at room temperature, the precursor was found to dissolve in the amine and a color change was observed. Subsequently, a minimum amount of ethanol was added to quench the reaction and PbS solid was isolated by centrifugation. The solid was then washed with ethanol and acetone and dried under vacuum. No reaction was found between PbTB and trioctylamine, as the precursor remained insoluble after being stirred for a long time in this amine.

(D) Preparation of PbS Nanodendrites from Bifunctional Ethylenediamine. PbTB (15 mg, 0.03 mmol) was added into a flask, followed by the injection of 4 mL (60 mmol) of ethylenediamine (EDA). After the solution was stirred for 15 min, ethanol was added to quench the reaction and solid was isolated by centrifugation. The solid was then washed with ethanol and acetone and dried under vacuum.

(E) Preparation of PbS Nanorods from Dodecanethiol and Ethylenediamine. A typical reaction was as follows: 2 mL of EDA (30 mmol) and a certain amount of dodecanethiol were mixed well and then added into a flask containing 15 mg of PbTB under vigorous stirring. After 15 min, ethanol was added to induce precipitation. The remaining treatments are the same as in the above-mentioned procedure.

(F) Characterization. Thermogravimetric analysis (TGA) was recorded on a SDT 2960 Simultaneous DTA-TGA. Approximately 10 mg of the precursor was decomposed under inert N_2 flow (90 mL/min) and a heating rate of 10 deg/min was used. Powder X-ray diffraction (XRD) patterns of the nanocrystals were recorded on a Siemens D5005 X-ray powder diffractometer with Cu Kα radiation (40 kV, 40 mA). The powdered sample was mounted on a sample holder and scanned with a step size of $2\theta = 0.01°$ in the range 20−60°. Transmission electron micrographs (TEM) were obtained with a 300 kV Philips TEM microscope. The samples were prepared by placing a drop of the nanocrystals dispersed in acetone onto a copper grid coated with carbon film and allowing them to dry in desiccators.

Results and Discussions

(A) Decomposition of the PbTB Precursor. The PbTB precursor is a crystalline pale yellow solid that is soluble in solvents such as DMF and DMSO. It is air-stable and relatively easy to prepare and purify, and can be stored in the dark for extended periods of time. As shown in Figure 1, TGA results indicated that decomposition of PbTB began at above ~178 °C, giving 49.1% residue at 345 °C. The decomposition profile is simple although a small bump is observed at ~300 °C. It is reasonable to predict that the organic $(C_6H_5OC)_2S$ fragment was removed eventually, leaving inorganic PbS residue in the condensed phase:

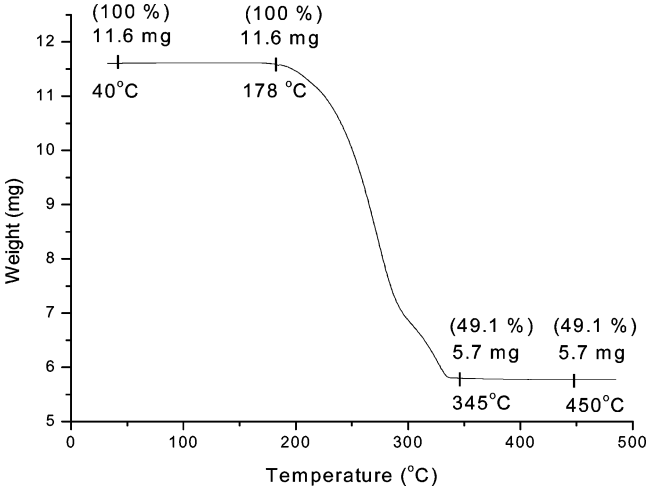

Figure 1. TGA curve of the $Pb(SCOC_6H_5)_2$ precursor.

$$Pb(SCOC_6H_5)_2 \xrightarrow[\Delta]{} PbS + (C_6H_5CO)_2S$$

The calculated weight percent for the PbS residue by the above chemical equation is 50.0%, which is in good agreement with the value given by TGA.

On the basis of the above TGA result, one would thus propose to prepare PbS nanocrystals by heating this precursor to temperatures above ~170 °C, typically using the injection method into solvents such as TOPO. Nevertheless, we describe here a new preparation route operative at room temperature. We have found that the PbTB precursor readily dissolves and decomposes by simply stirring it in amine at room temperature. When a short-chain amine such as ethylamine or propylamine was used, large crystals precipitated immediately with stirring. On the other hand, we found that uniform 5−10 nm spherical PbS nanocrystals can be optimally produced quantitatively when long-chain amines are used. We have further found that different morphology of PbS nanocrystals can be obtained when different amines or a mixture of reagents is utilized. A summary of our findings is given in Table 1, and the detailed results are discussed in the following subsections B−D.

TABLE 1: A Summary of the Size and Shape of PbS Nanocrystals Prepared at Room Temperature

amine used[a]	reaction time (min)	morphology	av dimensions[b] (nm)
ethylamine	5	spherical	$D = 60 \pm 6.7$
OLA	30	spherical	$D = 8.9 \pm 1.7$
dioctylamine	30	spherical	$D = 5.9 \pm 0.6$
EDA	15	dendrites	trunks ($W = 50 \pm 11$, $L = 400$) sticks ($W = 20 \pm 4$)
PbTB:DDT = 1:1	10	nanorods	$W = 60-120$ $L = 1000-3000$
PbTB:DDT = 1:2	10	nanowires	$W = 70-110$ $L = 1000-5000$
PbTB:DDT = 1:10	10	spherical	$D = 5.2 \pm 0.4$
ethylamine + EDA	15	mixture of nanorods, dendrites, spherical particles	
trioctylamine or triethylamine	>600	no reaction	

[a] OLA = oleylamine; EDA = ethylenediamine; DDT = dodecanethiol. [b] D = diameter; W = width; L = length.

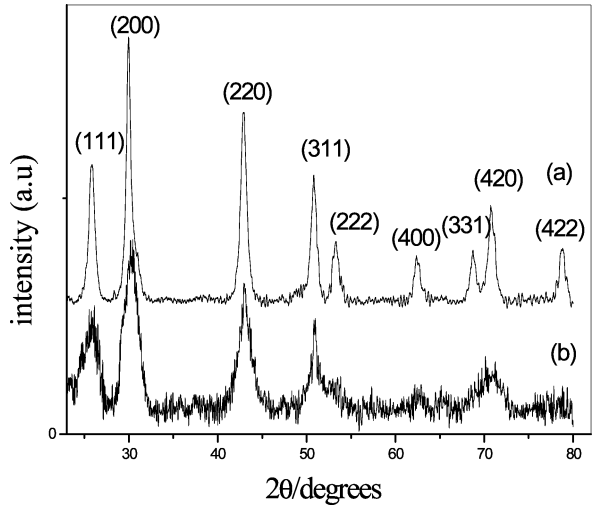

Figure 2. Typical XRD patterns of PbS nanocrystals prepared with (a) *n*-oleylamine and (b) dioctylamine.

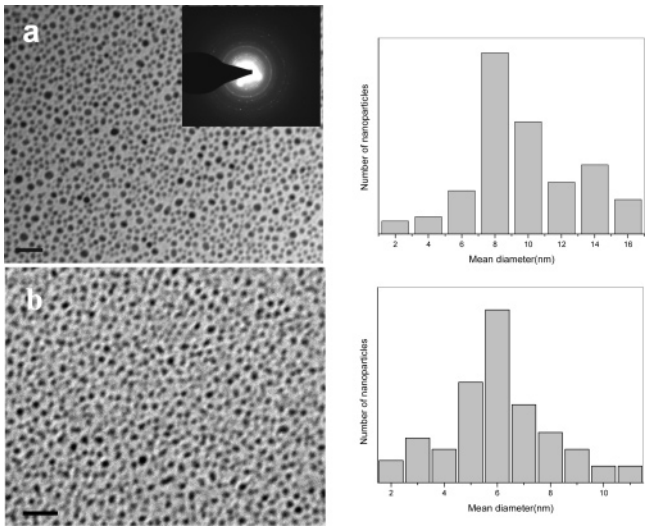

Figure 3. TEM images, size histograms, and selected area diffraction patterns (SAED) of the PbS nanocrystals: (a) *n*-oleylamine and (b) dioctylamine. Scale bar = 50 nm.

(B) Formation of Spherical PbS Nanocrystals at Room Temperature. As mentioned above, the PbTB precursor was found to readily decompose by stirring it with amine at room temperature. Figure 2 shows the typical wide-angle XRD pattern of the products, which confirms diffraction peaks indexed to the cubic rock-salt structure of the bulk galena PbS phase (JCPDS 5-592). The broadness in the observed diffraction peaks is characteristic of nanosized particles, but the crystalline nature of the product obtained at room temperature is clearly demonstrated. Estimation following the Debeye−Scherrer equation[26] gave average particle sizes of 9.8 nm (*n*-oleylamine, OA) and 6.0 nm (dioctylamine, DOA) respectively from the average broadening of the (200) and (220) peaks. The reaction with amines was found to be a general one: i.e., shorter alkylamines such as ethylamine, propylamine, or diethylamine also catalyze the reaction at room temperature, but the PbS particles formed are large and quickly aggregate to the bottom of the flask. On the other hand, longer chain amines such as OA, DOA, or OLA produce uniform spherical PbS nanocrystals readily.

Typical TEM images in Figure 3 show the nearly spherical PbS nanocrystals obtained, together with the respective size distribution histograms. The average particle size is estimated (counting ~100 particles in each case) as 8.9 ± 1.7 and 5.9 ± 0.6 nm, for OLA- and DOA-capped particles, respectively. These values fit very well with those determined from XRD. The selected-area electron-diffraction pattern (SAED) of the nanocrystals is consistent with the cubic phase of PbS ring patterns showing (111), (200), (220), (311), (221), and (400) planes. Since our preparation is performed at room temperature, particle size and monodispersity can be conveniently optimized by varying just two factors, i.e., the type of amines used and the amine-to-precursor ratio.

To understand the role of amine in our preparation, we have also attempted the reaction using different types of commonly used capping reagents such as thiols and carboxylic acids. At room temperature, however, PbTB showed no sign of decomposition when stirred in these reagents for long periods of time. Injecting PbTB into these reagents at elevated temperatures (typically >100 °C) does induce its decomposition, but only resulted in the precipitation of bulk PbS solids.

Expectedly, heating the alkylamines up to 80 °C before the injection of PbTB will induce faster growth of the PbS nanocrystals. The reaction has to be quenched very quickly when heated, however, or else bulk PbS solids will soon precipitate from the mixture. We have also noted that the formation of PbS nanocrystals occurs with OA and DOA, but not with trioctylamine. It thus seems that amine with an active hydrogen atom is important in effecting the reaction. In addition, OA seems to induce higher growth rate and thus produce nanocrystals with more polydispersed sizes as compared to DOA. Longer primary amines such as OLA, on the other hand, could produce better and more uniform nanocrystals compared to OA (Table 1).

On the basis of the above observations, we believe that the formation of PbS nanocrystals from PbTB precursor is not a simple thermolysis process. Most probably, the primary and secondary amines have acted as nucleophiles[27] and attack the electron-deficient (i.e., electrophilic) carbonyl carbon of the thiocarboxylate precursor in the initial step. This is followed by an elimination reaction to form PbS monomer together with byproducts such as amide and thiol:

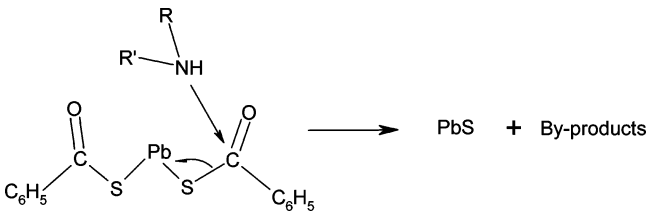

To further investigate this proposal, we have performed DFT B3LYP//LANL2DZ transition state calculations on the modeled system.[28] Indeed, optimization confirms a transition state structure with clear breaking of one C−S bond and the formation of a C−N bond as shown in Figure 4. The reaction is predicted to be exothermic with an enthalpy change of −17.2 kJ mol^{-1}, and the calculated energy barrier is 92.8 kJ mol^{-1} after zero-point correction. The low energy barrier thus confirms our proposition of an initial nucleophilic attack by amine that leads to the decomposition of PbTB at room temperature.

We expect the so-produced PbS monomers to nucleate and grow rapidly into larger crystals in view of the low solubility constant of PbS ($K_{sp} = 8 \times 10^{-28}$).[29] Meanwhile, free surrounding amine molecules will passivate the surfaces of the growing crystals. Hence, amine is playing the role of both a nucleophile and a capping agent in this preparation. While the shorter chain amines are less efficient in capping and thus tend

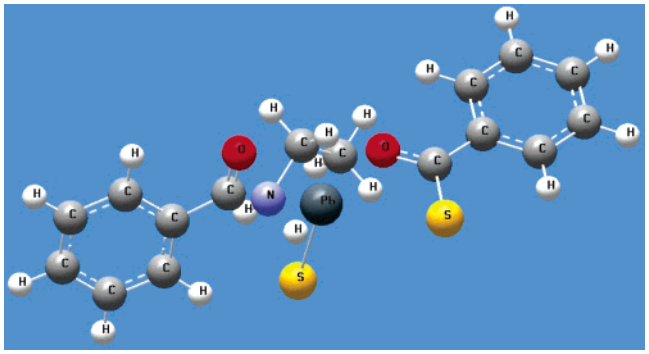

Figure 4. DFT B3LYP//LANL2DZ optimized transition state structure for the initial attack of amine (shown here as ethylamine) on PbTB. The two Pb−S bonds are respectively 2.54 and 2.93 Å, the breaking C−S bond is 2.75 Å while the newly formed C−N bond is 1.57 Å in the transition state.

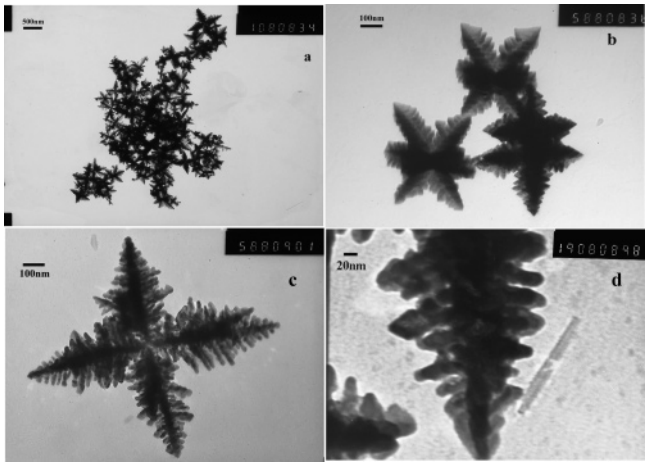

Figure 5. TEM images of PbS dendrites: (a) a typical area of the sample, (b) a six-armed structure, (c) a four-armed structure, and (d) one of the "sticks" with higher magnification.

to produce bulk PbS solids, the longer chain amines give good capping ability and stabilize the PbS nanocrystals.

The dual role of amine is manifested in the formation of smaller and more monodispersed nanocrystals from DOA as compared to OA (Table 1). Two plausible explanations can be offered to account for these differences. First, the primary OA has less hindrance and thus can attack the precursor more easily in the initial step. Second, since the amines are also acting as capping agent, the bulkier DOA is expected to play a better role to prevent the PbS crystals from aggregation and thus giving more monodispersed nanocrystals.

In short, we report here a method to prepare PbS nanocrystals very conveniently by catalyzing the decomposition of PbTB precursor at room temperature. We noted that monofuntional amines could produce PbS nanocrystals of spherical shape in fairly good size distribution (±10−15%) without the need of size-selection. In the following sections, we illustrate a simple method to modify the morphology of these nanocrystals at room temperature.

(C) Formation of PbS Dendrites at Room Temperature. We found that the above reaction can also occur at room temperature when ethylenediamine (EDA) was used. In this case, nevertheless, TEM analysis indicated that dendritic PbS nanostructures are exclusively produced. Figure 5 shows typical TEM images of the dendrites formed and it can be clearly seen that the dendrites are made up of either six- (Figure 5b) or four-armed (Figure 5c) structures. Each of these arms contains a main "trunk" with smaller "sticks" growing parallel from its length

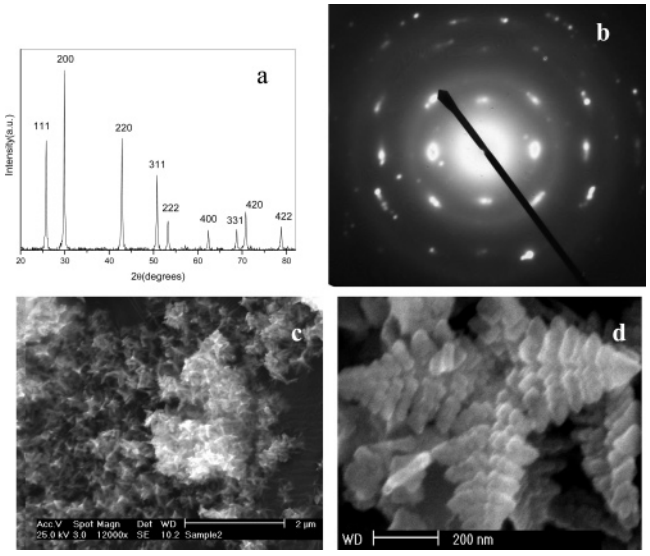

Figure 6. Typical XRD (a) and SAED (b) pattern indicating the rock salt structure of the PbS dendrites. (c and d) SEM micrographs of the dendrites.

(the structure is sometimes described as "fish bones"). The average diameter and length of the "trunk" are ca. 50 and 400 nm respectively. From the close-up image in Figure 5d, it can be seen that while the width of these sticks remains ∼20 nm, their length decreases linearly from tens of nanometers to several nanometers.

The crystallinity of the as-prepared dendrites is clearly illustrated by its distinct XRD and SAED patterns shown in Figure 6. The sharp cubic rock salt XRD pattern gives a lattice parameter of $a = 5.924$ Å, in good agreement to the JCPDS 5-592 database. The abundance of PbS dendrites produced with this method is illustrated in the SEM images in Figure 6, parts c and d.

After repeating the experiment many times, we conclude that PbS dendrites are always produced regardless of the relative molar ratio of EDA and PbTB used. There is also no clear relationship between molar ratio and the dimensions of the dendrites obtained. The reaction occurs rapidly and can be completed within ∼15 min. We have also attempted to investigate the morphological evolution of these dendrites by withdrawing samples at different time intervals for TEM analysis (Figure 7). It appears that spherical seeds are initially formed, but the growth of these seeds to dendrites is fairly rapid. Thus, while some near-spherical structures are still observable at 5 min after mixing (Figure 7b), the particles have grown into full 4- or 6-armed dendrites at ∼12 min (Figure 7d). Since the reaction occurs rapidly at room temperature, such morphological development would best be monitored by in situ microscopic observation.

To further understand the role of EDA in our preparation, we attempted the reaction using other bifunctional amines of different chain lengths such as 1,3-propylamine, 1,4-butylamine, and 1,6-hexylamine. There was no dendrite formation in these cases; however, only quasicubic or irregularly shaped nanoparticles were produced. Thus, it appears that the more rigid EDA molecule is crucial for the growth of dendritic morphology. On the other hand, when other bidentate ligands such as 1,2-ethanedithiol or oxalic acid solution were used, no reaction would occur at room temperature even after the mixture was kept overnight.

From the above observations, one would thus propose that the formation of dendrites is related to the bidendate cis-

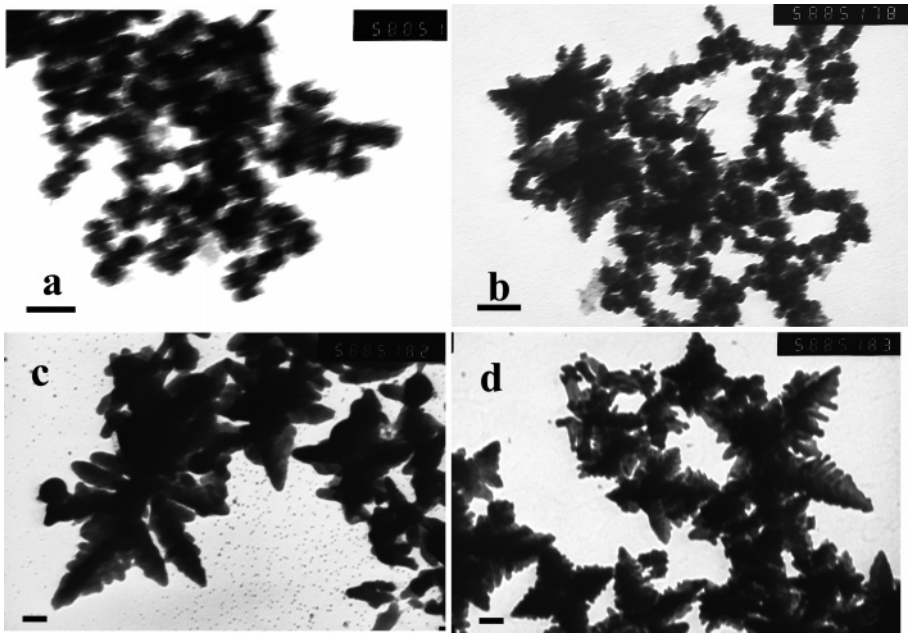

Figure 7. TEM images showing the growth of PbS dendrites at (a) 3, (b) 5, (c) 8, and (d) 12 min after the mixing of reagents. Scale bar = 100 nm.

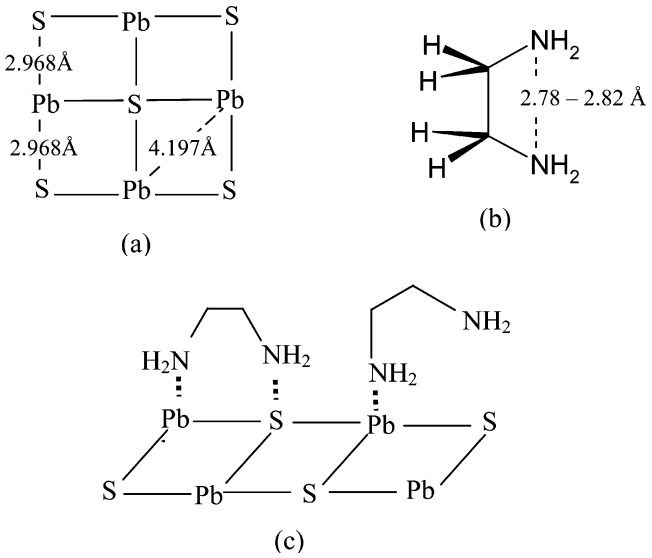

Figure 8. (a) The (100) plane of a unit cell of the PbS rock salt structure and the various interatomic distances, (b) the coplanar structure of an EDA molecule in the cis configuration, and (c) the monodendate and bidendate coordination configuration of EDA onto the PbS crystal facet.

coordination ability of EDA. In a growing nanoseed, the EDA molecule can cap in a cis configuration onto the facets of the crystal (Figure 8a). Other diamines with longer chain length will not readily form a stable cis configuration due to the higher entropy factor. In the cis conformation, our DFT modeling suggested that the interatomic distance between the two N atoms of EDA is 2.78−2.82 Å apart for dihedral angle ∠NCCN within 0−30°. The side of a PbS cubic rock salt unit cell is known to be 5.936 Å,[29] giving the interatomic distance between Pb and adjacent S atom as 2.968 Å. The shortest distance between two Pb atoms is the diagonal, which is calculated to be 4.197 Å. Thus, it seems that, in a bidendate configuration, the two $-NH_2$ groups of EDA would have to coordinate to one Pb and one S atom simultaneously (Figure 8c).

Of course we envisage that the EDA molecule could also cap in a monodendate manner onto either the Pb or the S atom. In this manner, one of the NH_2 groups will be extending out and may thus attach onto other growing nanocrystals. Since the interatomic distances match rather well, this will thus facilitate oriented attachment of the nanocrystals onto the growing crystals and hence induce the dendrite formation.

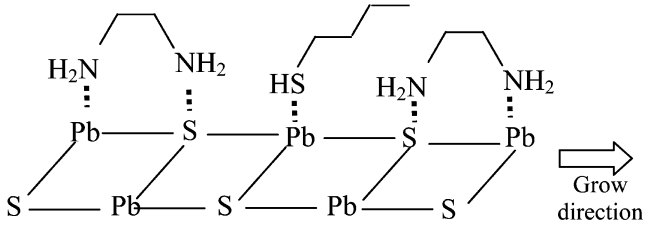

Figure 9. Schematic diagram showing the unidirectional growth of PbS when the monodendate EDA molecule is replaced by the stronger-binding thiol molecule. Only one row is illustrated for the purpose of clarity.

To elucidate the above proposal, we added a small amount of mononfunctional amine such as propylamine or diethylamine into the EDA preparation. This should inhibit oriented attachment since there is now competing capping from the monofunctional amines. Indeed, we observed spherical nanoparticles together with a small amount of irregular dendrites from these controlled reactions. Interestingly, some nanorods appear to coexist among the spherical and dendritic nanocrystals. Such unidirectional 1D crystal growth is not observed when the ratio of the amines is reversed, i.e., a small amount of EDA was added into a preparation using monofunctional amine.

(D) Inducing the Growth of PbS Nanorods at Room Temperature. Thus, on the basis of the above observation, we suggest that unidirectional growth of PbS may be achieved if a reagent that has higher capping affinity than amine is added together with EDA. This is because one will expect the monodendate EDA molecules to be readily replaced by these stronger capping groups, while EDA molecules bound in the bidentate manner will be energetically less readily replaced. Thus, oriented attachment to form "sticks" will be impeded and the "trunks" will continue to grow in a unidirectional manner (Figure 9).

Indeed, when a small amount of dodecanethiol (DDT) was added into the EDA preparation, we found that exclusively

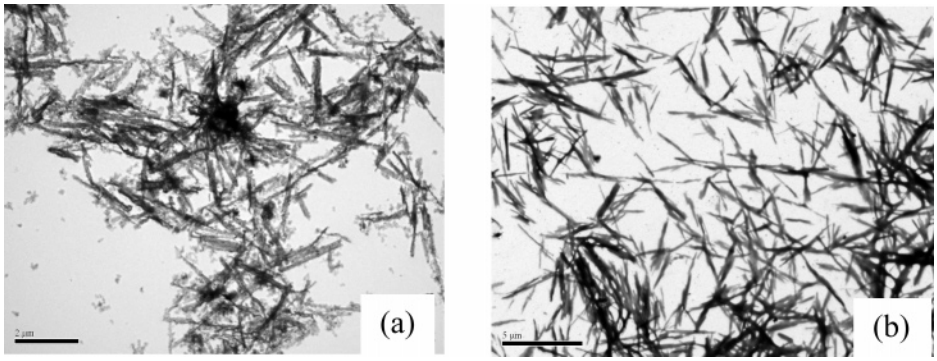

Figure 10. PbS nanorods/nanowires obtained from mixtures with various thiol-to-precursor molar ratios: (a) ratio = 1:1, diameter = 60−120 nm, length = 1000−3000 nm, and scale bar = 2 μm, and (b) ratio = 2:1, diameter = 70−110 nm, length = 1000−5000 nm, and scale bar = 5 μm.

nanorods or nanowires were obtained (Figure 10). The aspect ratio of these 1D crystals seems to be affected slightly by the relative ratio between PbTB and the thiol capping reagent. When the molar ratio of thiol-to-PbTB exceeds 10, however, only spherical PbS nanocrystals were obtained again. This is expected since the thiol group, having higher capping affinity, will then dominant and control the growth process. Thus, optimizing the relative amount of the two reagents is essential for a balance in control of the morphology of the prepared nanocrystals.

In conclusion, a simple route has been developed to prepare PbS nanocrystals in controlled morphology utilizing PbTB precursor at room temperature. The amines were used both as the catalyst and as the growth-control reagent in this preparation. We have demonstrated an elegant way of chemically controlling the growth morphology of the nanocrystals using different amines or mixtures of capping groups. By altering the affinity of capping agents to the growing nanoseeds, it is possible to control the size and shape of the final products. In addition, the growth mechanism for the generation of these nanocrystals has been demonstrated.

Acknowledgment. This research work was supported by a National University of Singapore research grant (Grant no. R-143-000-167-112). We thank Mr Wong Chiong Teck for his assistance in performing the DFT calculations.

References and Notes

(1) Hatzor, A.; Weiss, P. S. *Science* **2001**, *291*, 1019.

(2) Huynh, W. U.; Dittmer, J. J.; Alivisatos, A. P. *Science* **2002**, *295*, 2425.

(3) Yan, H. Q.; He, R. R.; Johnson, J.; Law, M.; Saykally, R. J.; Yang, P. D. *J. Am. Chem. Soc.* **2003**, *125*, 4728.

(4) Manna, L.; Milliron, D. J.; Meisel, A.; Scher, E. C.; Alivisatos, A. P. *Nat. Mater.* **2003**, *2*, 382.

(5) Peng, X. G.; Manna, L.; Yang, W. D.; Wickham, J.; Scher, E. C.; Kadavanich, A.; Alivisatos, A. P. *Nature* **2000**, *404*, 59.

(6) Peng, Z. A.; Peng, X. G. *J. Am. Chem. Soc.* **2001**, *123*, 1389.

(7) Jun, Y. W.; Lee, S. M.; Kang, N. J.; Cheon, J. *J. Am. Chem. Soc.* **2001**, *123*, 5150.

(8) (a) Mukherjee, M.; Datta, A.; Chakravorty, D. *Appl. Phys. Lett.* **1994**, *64*, 1159. (b) Subramanian, V.; Murali, K. R.; Rangarajan, N.; Lakshmanan, A. S. *Proc. SPIE. Int. Soc. Opt. Eng.* **1994**, *2274*, 219.

(9) Ellingson, R. J.; Beard, M. C.; Johnson, J. C.; Yu, P.; Micic, O. I.; Nozik, A. J.; Shabaev, A.; Efros, A. L. *Nano Lett.* **2005**, *5*, 865.

(10) Schneider, T.; Haase, M.; Kornowski, A.; Naused, S.; Weller, H.; Forster, S.; Antonitti, M. *Ber. Bunsen-Ges. Phys. Chem.* **1997**, *101*, 1654.

(11) Parvathy, N. N.; Pajonk G. M.; Rao, A. V. *J. Cryst. Growth* **1997**, *179*, 249.

(12) Lipovskii, A. A.; Kolobkova, V. E.; Olkhovets, A.; Petrikov, V.; Wise, F. *Phys. E* **1999**, *5*, 157.

(13) Konopny, L.; Berfeld, M.; Biro, R. P.; Weissbuch, I.; Leiserowitz, L.; Lahav, M. *Adv. Mater.* **2001**, *13*, 580.

(14) (a) Wang, Y.; Suna, A.; Mahler, W.; Kawoski, R. *J. Chem. Phys.* **1987**, *87*, 7315. (b) Kane, R. S.; Cohen, R. E.; Silbey, R. *Chem. Mater.* **1996**, *8*, 1919. (c) Dutta, A. K.; Ho, T. T.; Zhang, L. Q.; Stroeve, P. *Chem. Mater.* **2000**, *12*, 1042.

(15) Trindade, T.; O'Brien, P.; Zhang, X.; Motevalli, M. *J. Mater. Chem.* **1997**, *7*, 1011.

(16) Hines, M. A.; Scholes, G. D. *Adv. Mater.* **2003**, *15*, 1844.

(17) Joo, J.; Na, H. B.; Yu, T.; Yu, J. H.; Kim, Y. W.; Wu, F. X.; Zhang, J. Z.; Hyeon, T. *J. Am. Chem. Soc.* **2003**, *125*, 11100.

(18) Bakueva, L.; Gorelikov, I.; Musikhin, S.; Zhao, X. S.; Sargent, E. H.; Kumacheva, E. *Adv. Mater.* **2004**, *16*, 926.

(19) (a) Mo, M. S.; Shao, M. W.; Hu, M. M.; Yang, L.; Yu, W. C.; Qian, Y. T. *J. Cryst. Growth* **2002**, *244*, 364. (b) Wang, W.; Geng, Y.; Qian, Y. T.; Ji, M.; Liu, X. *Adv. Mater.* **1998**, *10*, 1479.

(20) Lee, S. M.; Jun, Y.; Cho, S.-N.; Cheon, J. *J. Am. Chem. Soc.* **2002**, *124*, 11244.

(21) (a) Kuang, D. B.; Xu, A. W.; Fang, Y. P.; Liu, H. Q.; Frommen, C.; Fenske, D. *Adv. Mater.* **2003**, *15*, 1747. (b) Ma, Y.; Qi, L.; Ma, J.; Cheng, H. *Cryst. Growth Des.* **2004**, *4*, 351,

(22) Ni, Y.; Liu, H.; Wang, F.; Liang, Y.; Hong, J.; Ma, X.; Xu, Z. *Cryst. Growth Des.* **2004**, *4*, 759.

(23) Lim, W. P.; Zhang, Z. H.; Low, H. Y.; Chin, W. S. *Angew. Chem., Int. Ed.* **2004**, *43*, 5685.

(24) Zhang, Z. H.; Vittal, J. J.; Chin, W. S. *J. Phys. Chem. B* **2004**, *108*, 18569.

(25) Burnett, T. R.; Dean, P. A. W.; Vittal, J. J. *Can. J. Chem.* **1994**, *72*, 1127.

(26) Azaroff, L. V. *X-ray diffraction*; Mcgraw-Hill: New York, 1974.

(27) Ahluwalia, V. K.; Parashar, R. K. *Organic Reaction Mechanisms*; CRC Press: Boca Raton, FL, 2002.

(28) Calculations were performed with the hybrid density functional B3LYP method and the effective core potential LANL2DZ basis set, using the Gaussian 98 suite of programs. Details of computational methodology may be found in the following: (a) Lee, C.; Yang, W.; Parr, R. G. *Phys. Rev. B* **1988**, *37*, 785. (b) Becke, A. D. *J. Chem. Phys.* **1993**, *98*, 5648. (c) Dunning, T. H., Jr.; Hay, P. J. in *Modern Theoretical Chemistry*;. Schaefer, H. F., III, Ed.; Plenum: New York, 1976; pp 1−28. (d) Hay, P. J.; Wadt, W. R. *J. Chem. Phys.* **1985**, *82*, 299.

(29) Bailar, J. C.; Emeleus, H. J.; Nyholm, S. R.; Trotman-Dickenson, A. F. *Comprehensive Inorganic Chemistry*; Pergamon Press: Elmsford, NY, 1973.